Crystal Structure Determination and Strain Analysis of Cobalt(III) and Copper(II) Complexes of Hexadentate and Tetradentate Ligands Containing Pyridyl Arms

JEFFREY B. MANDEL and BODIE E. DOUGLAS*

Department of Chemistry, University of Pittsburgh, Pittsburgh, PA 15260, U.S.A.

(Received May 17, 1988)

Abstract

Crystal structures of the novel complexes [Co(edampda)]$BF_4 \cdot H_2O$ (edampda is *N,N'*-bis(2-pyridylmethyl)ethylenediamine-*N,N'*-diacetate) (triclinic, $P\bar{1}$, $a = 7.893(3)$, $b = 11.415(5)$, $c = 12.421(5)$ Å, $\alpha = 110.42(3)°$, $\beta = 96.44(3)°$, $\gamma = 92.10(3)°$, $V = 1038.8(6)$, $Z = 2$, $D_{calc} = 1.61$, $R = 0.039$ for 3481 observed reflections) and [Cu(*uns*-Hpenp)Cl_2]ClO_4 (*uns*-Hpenp is *N,N*-bis(2-pyridylmethyl)-1-aminoethylammonium) (orthorhombic, *Pcam*, $a = 15.220(2)$, $b = 7.946(4)$, $c = 14.953(5)$ Å, $V = 1808.4(8)$, $Z = 4$, $D_{calc} = 1.75$, $R = 0.051$ for 1459 observed reflections) have been determined. Also, crystal structures of the complexes [Co(tpen)]$(ClO_4)_3$ (tpen is *N,N,N',N'*-tetrakis(2-pyridylmethyl)-ethylenediamine) (monoclinic, $P2_1/c$, $a = 9.748(6)$, $b = 18.27(1)$, $c = 19.98(1)$ Å, $\beta = 115.95(4)°$, $V = 3199(3)$, $Z = 4$, $D_{calc} = 1.62$, $R = 0.101$ for 2767 observed reflections), [Co(tppn)]$(ClO_4)_3$ (tppn is *N,N,N',N'*-tetrakis(2-pyridylmethyl)-1,2-propanediamine) (orthorhombic, $P2_12_12_1$, $a = 9.849(4)$, $b = 18.49(1)$, $c = 18.708(8)$ Å, $V = 3406(2)$, $Z = 4$, $D_{calc} = 1.55$, $R = 0.067$ for 2804 observed reflections), and tppn (triclinic, P_1, $a = 6.258(3)$, $b = 9.570(4)$, $c = 10.629(5)$ Å, $\alpha = 77.85(4)°$, $\beta = 88.82(3)°$, $\gamma = 74.22(3)°$, $V = 598.3(5)$, $Z = 1$, $D_{calc} = 1.22$, $R = 0.049$ for 1548 observed reflections) have been determined. The degree of strain in the chelate rings of the cobalt and copper complexes is analyzed via ring angle sum deviations from ideal ring angle sums. The degree of strain in these complexes is compared to the smaller degree of strain in the structurally analogous complexes of $[Co(edta)]^-$, $[Co(penten)]^{3+}$ and $[Co(\ell\text{-mepenten})]^{3+}$ (edta is ethylenediamine-*N,N,N',N'*-tetraacetate; penten is *N,N,N',N'*-tetrakis(2-aminoethyl)ethylenediamine; mepenten is *N,N,N',N'*-tetrakis(2-aminoethyl)-1,2-diaminopropane). The bond angles of the polypyridyl edampda, tpen and tppn complexes show large ligand–cobalt–ligand (L–Co–L) angles opposite to, and in the plane of, the ethylenediamine ring and systematically acute L–Co–L angles in some octahedral faces. The absolute configuration of $(-)_{589}$-[Co(tppn)]$(ClO_4)_3$ is identified as ΔΛΔ by analysis of Friedel pairs collected with Cu Kα radiation, and this absolute configuration is correlated to negative Cotton effects for three transitions observed in the circular dichroism spectrum. Finally, the crystal structure of [Cu(*uns*-Hpenp)Cl_2]ClO_4 unambiguously confirms the synthesis of the novel ligand, *uns*-penp (*uns*-penp is *N,N*-bis(2-pyridylmethyl)ethylenediamine).

Introduction

In recent decades, numerous crystallographic studies of cobalt complexes of aminopolycarboxylate ligands have been published; however, crystallographic studies of cobalt complexes of tetradentate and hexadentate polypyridyl ligands have been relatively rare. Therefore, this study was initiated to obtain crystallographic data for cobalt polypyridyl complexes and to analyze the degree of strain in polypyridyl cobalt complexes in comparison to aminopolycarboxylate cobalt complexes.

Pyridyl chelate arms induce much more strain in a metal complex than an acetate arm, for five-membered rings. The pyridine ring, containing two sp^2 atoms, induces planarity in the outer region of a pyridyl arm. This constraint is not present in an acetate arm which contains one sp^2 carbon. Analysis of ring angle sums for chelate rings provides an accurate measure for the total strain in these systems.

In addition to the structural studies of interest to a coordination chemist, heavy metal chelation by polypyridyl ligands is useful in biochemical studies. The ligand tpen (*N,N,N',N'*-tetrakis(2-pyridylmethyl)ethylenediamine) has recently been used as a heavy metal chelator in studies measuring free cytosolic Ca^{2+} in Ehrlich and Yoshida *Ascites carcinomas* [1]. Also tpen has recently been used in work investigating the effect of iron chelating agents on the toxicity of doxorubicin for MCF-7 human breast cancer cells [2].

*Author to whom correspondence should be addressed.

0020-1693/89/$3.50

The ability of lipid-soluble tpen to cross artificial and natural membranes and preferentially chelate intracellular heavy metals makes it a useful tool for investigating the roles of heavy metals inside cells. High affinities for heavy metals and low affinities for Mg^{2+} and Ca^{2+} also contribute to tpen's value. Studies conclude that further modification of tpen's structure is needed to increase its ability to discriminate between beneficial and toxic heavy metals [1]. Therefore, crystallographic studies of strain in various polypyridyl metal complexes are of potential biochemical importance.

The ligand tpen has appeared in a crystallographic study of a binuclear Cu(I) complex, $[Cu_2(tpen)](BF_4)_2$ [3], and the ligand tepen (*N,N,N'*-tris(2-(2-pyridyl)ethyl)ethylenediamine) was used in the crystallographic study of the nickel complex, $[Ni(tepen)](ClO_4)_2$ [4]. Finally, the tetradentate ligand tpa (tris(2-pyridylmethyl)amine) was used in the crystallographic study of $[Cu(tpa)Cl]PF_6$ [5].

Synthesis and Crystal Growth

The syntheses of the compounds in this work were reported by Mandel *et al.* [6]. The crystals of the tpen, tppn and edampda complexes were obtained by slow evaporation of water solutions. The origin of the crystals of the $[Cu(uns\text{-}Hpenp)Cl_2]^+$ complex was documented in the published synthesis [6]. The crystals of tppn were obtained by slow evaporation of a chloroform solution in an imperfectly sealed NMR tube.

Attempts to grow suitable single crystals of $[Co(edampda)]^+$ utilized numerous counterions: Cl^-, Br^-, I^-, PF_6^-, BF_4^- and ClO_4^-. Only the BF_4^- and ClO_4^- counterions produced usable single crystals of the edampda complex. Many of the $[Co(edampda)]BF_4$ and $[Co(edampda)]ClO_4$ crystals were twinned.

Attempts to grow suitable single crystals of $[Co(tpen)]^{3+}$ $(-)_{589}$-$[Co(tppn)]^{3+}$, and $[Co(tptn)]^{3+}$ utilized numerous counterions: Cl^-, Br^-, I^-, tartrate, NO_3^-, PF_6^-, BF_4^-, PO_4^{3-}, $S_2O_6^{2-}$, ClO_4^-, $[Co(\ell\text{-}cysu)_3]^{3-}$, $[Co(CN)_6]^{3-}$, $[Co(NO_2)_6]^{3-}$, $[Cr(ox)_3]^{3-}$, CF_3SO_3Ag, toluenesulfonate and 1,3,5-benzenetricarboxylate. All of the monoatomic counterions produced oils. Of the polyatomic counterions, only the BF_4^- and ClO_4^- anions produced usable single crystals. Preliminary refinements of structures of single crystals of $[Co(tpen)](BF_4)_3$ and $(-)_{589}$-$[Co(tppn)](BF_4)_3$ indicated that all of the BF_4^- anions were extremely disordered; therefore, crystal structures of the perchlorates of the tpen and tppn complexes were determined. Single crystals of $[Co(tptn)](ClO_4)_3$ and $[Co(tptn)](BF_4)_3$ were too thin for X-ray structure determination.

X-ray Crystallography

Procedure

Data were collected using graphite monochromated Mo Kα radiation ($\lambda = 0.71069$ Å) at 25 °C using $\theta/2\theta$ (bisecting) scans at a speed of 12°/min using a Nicolet R3m/E crystallographic system. The criterion for observation was $I > 2.5\sigma(I)$. Absorption corrections were calculated from a transmission curve based on a set of azimuthal scans. The absorption corrections were processed using the program XEMP supplied by Nicolet. Calculations were carried out with the SHELXTL package supplied by Nicolet. The scattering factors that were used were from ref. 7. The structures were refined by a least-squares procedure that utilized a 'blocked cascade' algorithm. The function minimized was $\Sigma w(|F_o| - |F_c|)^2$ where $w = 1/[\sigma^2(F_o) + gF_o^2]$. Weights were based on counting statistics with instrumental instabilities accounted for by a factor, g. This factor was initially refined and then constrained to a constant value in the final stages of the least-squares refinement. All non-hydrogen atoms were refined anisotropically.

Structure 1, [Co(edampda)]$BF_4 \cdot H_2O$ (edampda is N,N'-bis(2-pyridylmethyl)ethylenediamine-N,N'-diacetato) (Fig. 1)

The lattice parameters for **1** were refined by least-squares procedures using 15 reflections that varied between 10° and 15° in θ. These 15 reflections were obtained from a rapid preliminary scan.

The data that were utilized for structure determination were collected over a hemisphere (0, −13, −14; 9, 13, 14). Three standard reflections (0, −5, −2; 4, 0, 1; 0, 7, 1) were measured every 50 reflections. The applied decay corrections, based on the three standard reflections, ranged from 0.99 to 1.01. An absorption correction was applied using a set of azimuthal transmission curves collected for 29 reflections with χ from 60° to 120°. The applied absorption corrections ranged from 0.73 to 0.93.

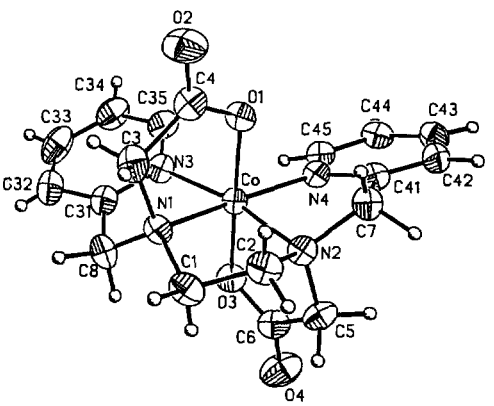

Fig. 1. An ORTEP diagram of $[Co(edampda)]^+$.

The Co position was located using Patterson methods, and the positions of the remaining atoms were determined from subsequent difference Fourier syntheses. Hydrogen atoms were located in difference Fourier maps and were refined isotropically.

The BF_4^- anion was disordered. One fluorine atom (F_1) was refined anisotropically with full occupancy. Each of the other fluorine atoms (F_2, F_3 and F_4) occupied three positions each with one-third occupancy. These disordered fluorine atoms were also refined anisotropically. One disordered water molecule was located in the difference Fourier map. This water molecule was distributed over two positions (w_1, 0.65; w_2, 0.35) and was refined anisotropically.

Structure 2, [Co(tpen)](ClO$_4$)$_3$ (tpen is N,N,N',N'-tetrakis(2-pyridylmethyl)ethylenediamine) (Fig. 2)

The lattice parameters for **2** were refined by least-squares procedures using 15 reflections that varied between 5° and 11° in θ. These 15 reflections were obtained from a rapid preliminary scan.

The data that were utilized for structure determination were collected over a quadrant (0, 0, −21; 10, 19, 21). Three standard reflections (0, 4, 3; 0, 0, −6; 3, 2, 0) were measured every 50 reflections. The applied decay corrections, based on the three standard reflections, ranged from 0.92 to 1.01. An absorption correction was applied using a set of azimuthal transmission curves collected for 30 reflections with χ from 240° to 300°. The applied absorption corrections ranged from 0.82 to 0.94.

The structure was solved using a combination of direct methods and subsequent difference Fourier syntheses. Difference syntheses revealed the positions of fifteen of the hydrogen atoms. The positions of the remaining hydrogen atoms were supplied by calculation. All hydrogen atoms were refined using an idealized model based on the atoms to which the hydrogen atoms are bonded.

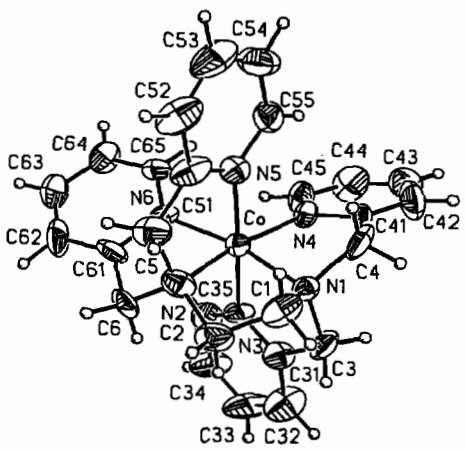

Fig. 2. An ORTEP diagram of $[Co(tpen)]^{3+}$.

The thermal vibrational parameters of many of the oxygen atoms of the three perchlorate anions were very large and significantly anisotropic. This indicated possible positional disorder; however, the observed electron density did not show any resolved disorder patterns around any of the three perchlorate anions. The anisotropy might be due to librational motion within the perchlorate counterions; therefore, a program that analyzes atomic thermal parameters in terms of molecular rigid body motion was used to determine if the perchlorate anions could be represented as rigid bodies [8, 9]. For all three perchlorate anions, the differences between the calculated and experimental anisotropic temperature factors were not statistically significant. (Perchlorate (**1**): $R_w = 0.052$, $GOF = 1.176$. Perchlorate (**2**): $R_w = 0.063$, $GOF = 1.568$. Perchlorate (**3**): $R_w = 0.053$, $GOF = 1.195$.) All of the Cl–O bond distances increased significantly after librational correction. The maximum correction was +0.18 Å; the average correction was +0.10 Å.

Overall, these analyses show that although some of the perchlorate oxygen temperature factors are unusually large, all three perchlorate counterions can be described satisfactorily as molecular rigid bodies undergoing mean-square-amplitude thermal vibrations.

Structure 3, ΔΛΔ-(−)$_{589}$-[Co(tppn)](ClO$_4$)$_3$ (tppn is N,N,N',N'-tetrakis(2-pyridylmethyl)-1,2-propanediamine) (Fig. 3)

The lattice parameters for **3** were refined by least-squares procedures using 15 reflections that varied between 10° and 12° in θ. These 15 reflections were obtained from a rapid preliminary scan.

The data that were utilized for structure determination were collected over an octant (0, 0, 0; 11, 22, 22). Three standard reflections (0, 6, 7; 4, 3, 5; 5, 3, 1) were measured every 50 reflections. The applied decay corrections, based on the three standard reflections, ranged from 0.85 to 1.00. An absorption correction was applied using a set of

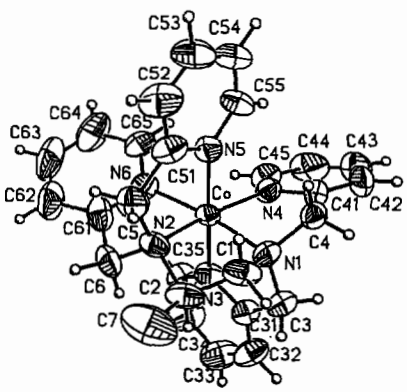

Fig. 3. An ORTEP diagram of $[Co(tppn)]^{3+}$.

azimuthal transmission curves calculated for 22 reflections with χ from 60° to 120°. The applied absorption corrections ranged from 0.59 to 0.61.

The Co position was located using Patterson methods, and the positions of the remaining non-hydrogen atoms were determined from subsequent difference Fourier syntheses. Difference syntheses revealed the positions of fifteen of the hydrogen atoms. The positions of the remaining hydrogen atoms were supplied by calculation. Hydrogen atoms were refined using an idealized model based on the atoms to which the hydrogen atoms are bonded. Hydrogen atoms were not generated for the methyl group.

Again, the thermal vibrational parameters of many of the oxygen atoms of the three perchlorate anions were very large and significantly anisotropic. This indicated possible positional disorder; however, once again, the observed electron density did not show any resolved disorder patterns around any of the three perchlorate anions. The anisotropy might be due to librational motion within the perchlorate counterions; therefore, the same program that was used for structure **2** was used to determine if the perchlorate counterions could be represented as rigid bodies [8, 9]. For all three perchlorate anions, the differences between the calculated and experimental anisotropic temperature factors were not statistically significant. (Perchlorate (**1**): $R_w = 0.044$, $GOF = 1.616$. Perchlorate (**2**): $R_w = 0.020$, $GOF = 0.730$. Perchlorate (**3**): $R_w = 0.071$, $GOF = 2.665$.) All of the Cl–O bond distances increased significantly after librational correction. The maximum correction was +0.17 Å; the average correction was +0.10 Å.

Overall, these analyses show that although some of the perchlorate oxygen temperature factors are unusually large, all three perchlorate counterions can be described satisfactorily as molecular rigid bodies undergoing mean-square-amplitude thermal vibrations.

The cobalt complex was also analyzed for rigid body motion. The comparison of the calculated anisotropic thermal parameters to the experimental values was good ($R_w = 0.105$, $GOF = 1.509$.) In this case, the corrections of the bond lengths for the cobalt complex were not statistically significant. The increase in bond length generally did not exceed the estimated standard deviation.

Friedel pairs were subsequently measured utilizing Cu Kα radiation (λ = 1.54178 Å) at 25 °C using the same Nicolet R3m/E crystallographic system.

Structure 4, [Cu(uns-Hpenp)Cl$_2$]ClO$_4$ (uns-Hpenp is N,N-bis(2-pyridylmethyl)-1-aminoethylammonium) (Fig. 4)

The lattice parameters for 4 were refined by least-squares procedures using 15 reflections that varied between 10° and 15° in θ. These 15 reflections were obtained from a rapid preliminary scan.

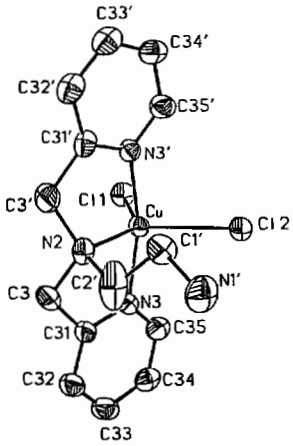

Fig. 4. An ORTEP diagram of [Cu(*uns*-Hpenp)Cl$_2$]$^+$.

The data that were utilized for structure determination were collected over an octant (0, 0, 0; 18, 9, 17). Three standard reflections (4, 0, 6; 0, 4, 4; 3, 3, 5) were measured every 50 reflections. The applied decay corrections, based on the three standard reflections, ranged from 0.97 to 1.00. An absorption correction was applied using a set of azimuthal transmission curves collected for 18 reflections with χ from 60° to 120°. The applied absorption corrections ranged from 0.41 to 0.45.

The systematic absences of reflections from the data set indicated the space group setting $Pca2_1$. The structure was determined using a combination of direct methods and subsequent difference Fourier synthesis assuming the space group $Pca2_1$. The structure was then found to be consistent with the higher symmetry space group *Pcam*, with the Cu complex making use of a crystallographic mirror plane and the perchlorate ion making use of a two-fold axis. The structure refinement was completed assuming space group *Pcam*.

The primary nitrogen of the ethylenediamine arm is not bonded to the Cu atom. Evidently, the pendant ethylenediamine arm nitrogen is protonated providing charge balance within the unit cell. The pendant ethylenediamine arm is disordered with respect to two conformations (Fig. 5). In each conformation, atoms C2, C1 and N1 with half occupancies are displaced on alternate sides of the mirror plane. The z parameters of atoms N1 and C2 were fixed to aid in the refinement.

Structure 5, tppn (tppn is N,N,N',N'-tetrakis(2-pyridylmethyl)-1,2-propanediamine) (Fig. 6)

The lattice parameters for **5** were refined by least-squares procedures using 15 reflections that varied between 10° and 14° in θ. These 15 reflections were obtained from a rapid preliminary scan.

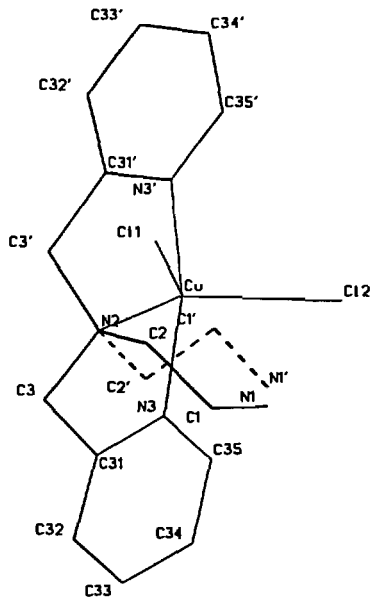

Fig. 5. A diagram of $[Cu(uns\text{-}Hpenp)Cl_2]^+$ showing both conformations of the pendant ligand arm.

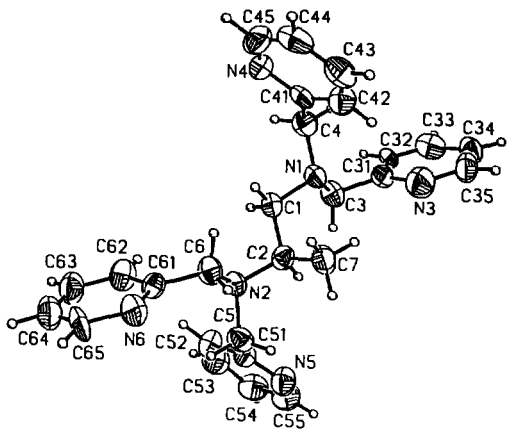

Fig. 6. An ORTEP diagram of tppn.

The data that were utilized for structure determination were collected over a hemisphere (0, −10, −11; 6, 10, 11). Three standard reflections (1, 0, 5; 1, 5, 0; 1, −3, −4) were measured every 50 reflections. The applied decay corrections, based on the three standard reflections, ranged from 0.97 to 1.01. An absorption correction was applied using a set of azimuthal transmission curves collected for 20 reflections with χ from 60° to 120°. The applied absorption corrections ranged from 0.91 to 0.95.

The structure was solved via a direct methods map which contained the positions of all of the non-hydrogen atoms. All hydrogen atoms were located using a combination of direct methods and subsequent difference Fourier syntheses. All hydrogen atoms were refined using an idealized model based on the atoms to which the hydrogens atoms are bonded.

Results and Discussion

Crystallographic parameters are given in Table 1. Atomic coordinates (Tables 2, 5, 8, 11, 14), bond lengths (Tables 3, 6, 9, 12, 15) and bond angles (Tables 4, 7, 10, 13, 16) are given for the four complexes and the ligand tppn.

The crystallographic data of the structure determinations show that the complexes $[Co(tpen)](ClO_4)_3$, $[Co(tppn)](ClO_4)_3$ and $[Co(edampda)]BF_4$ are significantly more strained than the previously studied complexes of analogous aminopolycarboxylate ligands. This increase in strain in these three complexes is due to the more rigid pyridyl arms. The ring strain in these three complexes will be compared to the ring strain in $[Co(penten)]^{3+}$, $[Co(\ell\text{-mepenten})]^{3+}$ and $[Co(edta)]^-$. $[Co(penten)]^{3+}$ is the aliphatic analog of $[Co(tpen)]^{3+}$ (penten is *N,N,N',N'*-tetrakis(2-aminoethyl)ethylenediamine). $[Co(\ell\text{-mepenten})]^{3+}$ is the aliphatic analog of $[Co(tppn)]^{3+}$ (mepenten is *N,N,N',N'*-tetrakis(2-aminoethyl)-1,2-diaminopropane). Finally, $[Co(edta)]^-$ is structurally analogous to the three cobalt complexes determined in this study (edta is ethylenediamine-*N,N,N',N'*-tetraacetate).

Weakliem and Hoard suggested that the sum of the bond angles of chelate rings could be used as an estimate of ring strain [10]. For example, the ideal sum of the bond angles of a five-membered glycinate ring is 538.5°. However, the sum of the bond angles in ring R_1 of $[Co(edampda)]^+$ is 537.8°. The difference in bond angle sums, Δ, is 0.7° and is a measure of ring strain.

Table 17 tabulates values of Δ for the hexadentate cobalt complexes of penten [11], ℓ-mepenten [12], edta [10], edampda, tpen and tppn. Table 17 also identifies the naming of the chelate arms in these complexes.

Using ring angle sum deviations from ideal ring angle sums, Weakliem and Hoard found that the G rings (in the plane of the ethylenediamine ring) in $[Co(edta)]^-$ were significantly more strained than the R rings (out of the plane of the ethylenediamine ring). This same trend is obvious for the complexes of edampda, tpen and tppn. However, the strain in the G pyridyl rings of the edampda, tpen and tppn complexes is approximately twice the strain in the G acetate rings of $[Co(edta)]^-$. This marked increase in strain in the G pyridyl arms of $[Co(edampda)]^+$, $[Co(tpen)]^{3+}$ and $[Co(tppn)]^{3+}$ is due to the planarity induced in the end of each G ligand arm from the two sp^2 atoms of the pyridine ring. The more highly puckered G acetate ring of $[Co(edta)]^-$ is less strained since it contains only one sp^2 atom.

TABLE 1. Crystallographic Parameters

	1	2	3	4	5
Formula	$CoC_{18}H_{20}N_4O_4BF_4 \cdot H_2O$	$CoC_{26}H_{28}N_6Cl_3O_{12}$	$CoC_{27}H_{30}N_6Cl_3O_{12}$	$CuC_{14}H_{19}N_4Cl_3O_4$	$C_{27}H_{30}N_6$
M	520.13	781.83	795.86	477.23	438.6
Color of crystal	red	orange	orange	blue	colorless
Crystal size (mm)	0.20 × 0.20 × 1.00	0.13 × 0.38 × 0.60	0.38 × 0.45 × 0.50	0.30 × 0.38 × 0.50	0.30 × 0.50 × 0.75
Calc. density (g/cm^3)	1.61	1.62	1.55	1.75	1.22
Crystal system	triclinic	monoclinic	orthorhombic	orthorhombic	triclinic
Space group	$P\bar{1}$	$P2_1/c$	$P2_12_12_1$	$Pcam$	$P1$
a (Å)	7.893(3)	9.748(6)	9.849(4)	15.220(2)	6.258(3)
b (Å)	11.415(4)	18.27(1)	18.49(1)	7.946(4)	9.570(4)
c (Å)	12.421(5)	19.98(1)	18.708(8)	14.953(5)	10.629(5)
α (°)	110.42(3)				77.85(4)
β (°)	96.44(3)	115.95(4)			88.82(3)
γ (°)	92.10(3)				74.22(3)
V (Å^3)	1038.8(6)	3199(3)	3406(2)	1808.4(8)	598.3(5)
Z	2	4	4	4	1
μ(Mo Kα) (cm^{-1})	8.90	8.55	8.05	16.85	0.70
2θ range	4–50	4–45	4–50	4–50	2–45
F(000)	512	1600	1632	972	234
Reflections measured	4231	4974	3627	1991	1856
Reflections rejected	25	98	20	10	30
Unique reflections	3690	4148	3375	1666	1718
Observed reflections	3481	2767	2804	1459	1548
Unobserved reflections	209	1381	571	207	170
R_{INT}	0.0105	0.0241			
max(Δ/σ)	−0.107	−0.445	−0.273	0.009	0.330
g	0.00200	0.00199	0.00377	0.00215	0.00423
Goodness of fit[a]	1.188	1.403	1.092	1.441	0.927
Residual density (e Å^{-3})	+0.73, −0.73	+1.09, −0.63	+0.83, −0.43	+0.72, −0.50	+0.18, −0.33
R_w	0.0440	0.0960	0.0713	0.0595	0.0550
R	0.0391	0.1007	0.0672	0.0510	0.0494

[a] $GOF = [\Sigma w(|F_o| - |F_c|)^2/m - n]^{1/2}$.

TABLE 2. Atomic Coordinates ($\times 10^4$) for [Co(edampda)]-$BF_4 \cdot H_2O$

	x	*y*	*z*
Co	2851(1)	2574(1)	3147(1)
N(1)	3224(2)	1367(2)	1662(2)
N(2)	2242(2)	1194(2)	3642(1)
C(1)	3299(3)	132(2)	1823(2)
C(2)	1940(3)	46(2)	2565(2)
C(3)	1741(3)	1347(2)	787(2)
C(4)	250(3)	1960(2)	1361(2)
O(1)	594(2)	2583(1)	2463(1)
O(2)	−1131(2)	1882(2)	795(2)
C(5)	3727(3)	1076(2)	4457(2)
C(6)	5297(3)	1902(2)	4495(2)
O(3)	5100(2)	2594(1)	3860(1)
O(4)	6607(2)	1892(2)	5098(2)
C(7)	713(3)	1540(2)	4251(2)
C(8)	4840(3)	1821(2)	1368(2)
N(3)	3771(2)	3765(2)	2485(1)
C(31)	4765(3)	3213(2)	1662(2)
C(32)	5622(3)	3897(3)	1137(2)
C(33)	5483(4)	5166(3)	1467(2)
C(34)	4443(3)	5722(2)	2282(2)
C(35)	3592(3)	4999(2)	2771(2)
N(4)	2138(2)	3569(2)	4629(1)
C(41)	1065(3)	2896(2)	5012(2)
C(42)	388(3)	3428(2)	6032(2)
C(43)	788(3)	4701(2)	6664(2)
C(44)	1872(3)	5381(2)	6271(2)
C(45)	2555(3)	4788(2)	5268(2)
B	2625(4)	1346(3)	7774(3)
F(1)	2479(2)	262(2)	8024(2)
F(2)	4156(5)	1373(4)	7254(4)
F(2′)	3365(16)	1268(11)	6927(7)
F(2″)	4110(7)	1646(5)	7575(9)
F(3)	1597(8)	1145(6)	6766(5)
F(3′)	1183(5)	1182(4)	6855(5)
F(3″)	1224(11)	1951(10)	7837(14)
F(4)	3795(12)	2073(6)	8790(6)
F(4′)	2516(8)	2378(5)	8744(4)
F(4″)	1898(11)	2320(7)	8486(5)
W(1)	9175(13)	3426(11)	9149(10)
W(2)	10375(41)	4171(22)	10285(25)

TABLE 3. Selected Bond Lengths (Å) for [Co(edampda)]-$BF_4 \cdot H_2O$

Co–N(1)	1.941(2)	Co–N(2)	1.944(2)
Co–O(1)	1.888(1)	Co–O(3)	1.889(2)
Co–N(3)	1.974(2)	Co–N(4)	1.954(2)
N(1)–C(1)	1.494(3)	N(1)–C(3)	1.499(3)
N(1)–C(8)	1.490(3)	N(2)–C(2)	1.498(2)
N(2)–C(5)	1.502(3)	N(2)–C(7)	1.488(3)
C(4)–O(1)	1.294(2)	C(3)–C(4)	1.511(3)
C(1)–C(2)	1.513(3)	C(4)–O(2)	1.212(3)
C(5)–C(6)	1.515(3)	C(6)–O(3)	1.298(3)
C(6)–O(4)	1.210(3)	C(7)–C(41)	1.502(3)
C(8)–C(31)	1.506(3)	N(3)–C(31)	1.351(3)
N(3)–C(35)	1.343(3)	C(31)–C(32)	1.381(4)
N(4)–C(45)	1.346(2)	C(32)–C(33)	1.373(4)
		C(33)–C(34)	1.371(4)
		C(34)–C(35)	1.380(4)
		N(4)–C(41)	1.353(3)
		C(41)–C(42)	1.378(3)
		C(42)–C(43)	1.393(3)
		C(43)–C(44)	1.372(4)
		C(44)–C(45)	1.375(3)

The G rings of $[Co(penten)]^{3+}$ and $[Co(\ell\text{-mepenten})]^{3+}$ are the least strained of these complexes since they contain no sp^2 atoms.

The strain in the R pyridyl arms of $[Co(tpen)]^{3+}$ and $[Co(tppn)]^{3+}$ is also markedly larger than the strain in the R acetate arms of both $[Co(edampda)]^+$ and $[Co(edta)]^-$ and ethylamine arm R_2 of $[Co(penten)]^{3+}$ and ethylamine arm R_1 of $[Co(\ell\text{-mepenten})]^{3+}$. (The chelate rings of the penten and ℓ-mepenten complexes adopt different conformations which accounts for the varying degrees of ring strain in their chelate arms.) Once again, the rigidity of the pyridyl arms causes ring strain to be introduced into the relatively planar R ligand arms.

In contrast, the strain within the R acetate arms of $[Co(edampda)]^+$ is, within experimental error, equal to the negligible strain of the R acetate arms of $[Co(edta)]^-$. The R acetate arms of $[Co(edampda)]^+$ are nearly planar as in $[Co(edta)]^-$. Therefore, the majority of the ring strain in $[Co(edampda)]^+$ is localized in the G pyridyl arms.

The ring strain in the E ring of $[Co(edampda)]^+$ is slightly larger than the ring strain in the E ring of $[Co(edta)]^-$. Further, the E ring strain in the more highly strained tpen and tppn complexes is approximately twice that in $[Co(edta)]^-$.

Table 18 tabulates values of root-mean-square deviations (RMSDs) of least-squares planes for the chelate rings of the complexes analyzed in this study. In general, the RMSDs show that R rings (acetate or pyridyl) are more planar than G rings (acetate or pyridyl) and that the magnitude of the RMSD of a least-squares plane of a chelate ring (R or G) is largely independent of pyridyl or acetate functionality. The RMSDs of the penten and ℓ-mepenten complexes do not distinguish between the chelate rings since they all adopt differing conformations. In general, the RMSDs of least-squares planes of chelate rings in cobalt complexes of hexadentate ligands can only distinguish between R and G rings and provide a measure of the overall degree of puckering in a chelate ring; the RMSDs of least-squares planes in cobalt complexes of hexadentate ligands do not provide a measure of the degree of strain in their corresponding chelate rings.

An interesting measure of the overall strain in these complexes is obtained by examining the L_G–Co–L_G angle in all four complexes. This angle is

TABLE 4. Selected Bond Angles (°) for $[Co(edampda)]BF_4 \cdot H_2O$

N(1)–Co–N(2)	89.3(1)	N(1)–Co–O(1)	86.9(1)
N(2)–Co–O(1)	92.8(1)	N(1)–Co–O(3)	94.3(1)
N(2)–Co–O(3)	87.4(1)	O(1)–Co–O(3)	178.8(1)
N(1)–Co–N(3)	82.0(1)	N(2)–Co–N(3)	169.3(1)
O(1)–Co–N(3)	92.8(1)	O(3)–Co–N(3)	87.2(1)
N(1)–Co–N(4)	169.6(1)	N(2)–Co–N(4)	82.3(1)
O(1)–Co–N(4)	87.4(1)	O(3)–Co–N(4)	91.4(1)
N(3)–Co–N(4)	107.0(1)	Co–N(1)–C(1)	106.1(1)
Co–N(1)–C(3)	107.8(1)	C(1)–N(1)–C(3)	111.4(2)
Co–N(1)–C(8)	106.7(1)	C(1)–N(1)–C(8)	114.0(2)
C(3)–N(1)–C(8)	110.5(2)	Co–N(2)–C(2)	106.1(1)
Co–N(2)–C(5)	107.8(1)	C(2)–N(2)–C(5)	110.8(2)
Co–N(2)–C(7)	106.3(1)	C(2)–N(2)–C(7)	114.6(1)
C(5)–N(2)–C(7)	110.8(2)	N(2)–C(2)–C(1)	107.0(2)
C(32)–C(33)–C(34)	119.3(3)	C(3)–C(4)–O(1)	115.0(2)
N(2)–C(5)–C(6)	112.3(2)	O(1)–C(4)–O(2)	124.4(2)
N(1)–C(1)–C(2)	107.5(2)	C(5)–C(6)–O(3)	115.3(2)
N(1)–C(3)–C(4)	111.7(2)	O(3)–C(6)–O(4)	124.7(2)
C(3)–C(4)–O(2)	120.6(2)	Co–N(3)–C(31)	111.8(2)
Co–O(1)–C(4)	116.4(1)	C(31)–N(3)–C(35)	118.7(2)
C(5)–C(6)–O(4)	120.0(3)	C(8)–C(31)–C(32)	123.7(2)
Co–O(3)–C(6)	115.9(1)	Co–N(4)–C(41)	112.4(1)
N(2)–C(7)–C(41)	106.1(2)	C(41)–N(4)–C(45)	118.8(2)
N(1)–C(8)–C(31)	106.1(2)	C(7)–C(41)–C(42)	123.6(2)
Co–N(3)–C(35)	129.4(2)	C(42)–C(43)–C(44)	119.4(2)
C(8)–C(31)–N(3)	115.0(2)	Co–N(4)–C(45)	128.7(2)
N(3)–C(31)–C(32)	121.3(2)	C(7)–C(41)–N(4)	114.6(2)
C(31)–C(32)–C(33)	119.5(2)	N(4)–C(41)–C(42)	121.7(2)
C(33)–C(34)–C(35)	119.1(2)	C(41)–C(42)–C(43)	118.7(2)
N(3)–C(35)–C(34)	122.0(2)		
C(43)–C(44)–C(45)	119.2(2)		
N(4)–C(45)–C(44)	122.1(2)		

TABLE 5. Atomic Coordinates ($\times 10^4$) for $[Co(tpen)](ClO_4)_3$

	x	*y*	*z*
Co	8288(2)	7106(1)	2192(1)
N(1)	6472(9)	7694(4)	1726(5)
N(2)	7251(10)	6560(5)	2669(5)
C(1)	5226(13)	7287(7)	1788(7)
C(2)	5900(14)	7012(7)	2574(7)
C(3)	6650(14)	8417(6)	2112(6)
C(4)	6262(13)	7817(7)	951(6)
C(5)	6775(16)	5811(7)	2310(7)
C(6)	8389(13)	6444(7)	3447(6)
N(3)	9031(10)	7872(5)	2935(4)
C(31)	8104(12)	8419(7)	2831(6)
C(32)	8430(15)	9017(8)	3308(8)
C(33)	9807(15)	9009(8)	3919(8)
C(34)	10815(15)	8471(7)	4028(7)
C(35)	10424(13)	7902(8)	3515(6)
N(4)	8969(11)	7733(4)	1605(5)
C(41)	7792(14)	8046(5)	1015(6)
C(42)	8050(20)	8524(7)	557(8)
C(43)	9518(21)	8716(9)	702(9)
C(44)	10665(17)	8398(7)	1302(9)
C(45)	10398(13)	7896(7)	1758(7)
N(5)	7644(9)	6328(5)	1458(4)
C(51)	6971(12)	5759(6)	1618(7)
C(52)	6542(14)	5151(7)	1179(8)
C(53)	6837(15)	5107(8)	586(8)
C(54)	7491(14)	5672(7)	418(7)
C(55)	7900(13)	6279(7)	848(6)
N(6)	9962(9)	6477(4)	2801(5)
C(61)	9809(13)	6199(7)	3417(6)
C(62)	10952(15)	5782(7)	3928(7)
C(63)	12190(17)	5591(8)	3819(8)
C(64)	12283(14)	5831(7)	3184(7)
C(65)	11144(11)	6267(6)	2694(6)
Cl(1)	2229(4)	5988(2)	1042(2)
O(11)	3222(10)	6026(6)	703(5)
O(12)	1016(11)	5523(6)	652(6)
O(13)	3056(10)	5732(7)	1781(5)
O(14)	1669(13)	6676(6)	1071(7)
Cl(2)	5213(4)	2946(2)	1139(2)
O(21)	5573(14)	3322(7)	631(6)
O(22)	6299(15)	2541(10)	1643(10)
O(23)	3844(15)	2621(9)	817(7)
O(24)	4895(29)	3473(10)	1552(11)

(continued)

TABLE 5. *(continued)*

Cl(3)	6457(4)	4730(2)	4026(2)
O(31)	7960(11)	4969(6)	4390(6)
O(32)	5830(16)	4816(10)	3297(6)
O(33)	5615(16)	4944(13)	4370(9)
O(34)	6547(15)	3987(7)	4189(8)

TABLE 6. Selected Bond Lengths (Å) for $[Co(tpen)](ClO_4)_3$

Co–N(1)	1.926(8)	Co–N(2)	1.941(11)
Co–N(3)	1.934(9)	Co–N(4)	1.952(11)
Co–N(5)	1.939(9)	Co–N(6)	1.931(8)
N(1)–C(1)	1.475(17)	N(1)–C(3)	1.500(14)
N(1)–C(4)	1.487(16)	N(2)–C(2)	1.495(17)
N(2)–C(5)	1.520(15)	N(2)–C(6)	1.477(12)
C(1)–C(2)	1.498(19)	C(3)–C(31)	1.514(13)
C(4)–C(41)	1.500(19)	C(5)–C(51)	1.480(22)
C(6)–C(61)	1.481(19)	N(3)–C(31)	1.301(15)
N(3)–C(35)	1.347(12)	C(31)–C(32)	1.393(19)
C(32)–C(33)	1.363(16)	C(33)–C(34)	1.338(20)
C(34)–C(35)	1.391(19)	N(4)–C(41)	1.359(12)
N(4)–C(45)	1.323(17)	C(41)–C(42)	1.365(21)
C(42)–C(43)	1.375(28)	C(43)–C(44)	1.360(19)
C(44)–C(45)	1.395(22)	N(5)–C(51)	1.340(16)
N(5)–C(55)	1.350(18)	C(51)–C(52)	1.362(17)
C(52)–C(53)	1.338(26)	C(53)–C(54)	1.331(22)
C(54)–C(55)	1.352(18)	N(6)–C(61)	1.398(17)
N(6)–C(65)	1.318(16)	C(61)–C(62)	1.367(16)
C(62)–C(63)	1.361(25)	C(63)–C(64)	1.383(23)
C(64)–C(65)	1.369(15)		

TABLE 7. Selected Bond Angles (°) for $[Co(tpen)](ClO_4)_3$

N(1)–Co–N(2)	87.6(4)	N(1)–Co–N(3)	85.7(3)
N(2)–Co–N(3)	95.5(4)	N(1)–Co–N(4)	82.2(4)
N(2)–Co–N(4)	169.6(4)	N(3)–Co–N(4)	85.7(4)
N(1)–Co–N(5)	96.8(3)	N(2)–Co–N(5)	85.9(4)
N(3)–Co–N(5)	177.3(4)	N(4)–Co–N(5)	93.4(4)
N(1)–Co–N(6)	168.8(5)	N(2)–Co–N(6)	82.1(4)
N(3)–Co–N(6)	91.0(3)	N(4)–Co–N(6)	108.2(4)
N(5)–Co–N(6)	86.8(3)	Co–N(1)–C(1)	107.2(6)
Co–N(1)–C(3)	111.5(6)	C(1)–N(1)–C(3)	108.3(10)
Co–N(1)–C(4)	105.5(7)	C(1)–N(1)–C(4)	114.9(8)
C(3)–N(1)–C(4)	109.5(9)	Co–N(2)–C(2)	105.8(8)
Co–N(2)–C(5)	110.4(9)	C(2)–N(2)–C(5)	111.5(9)
Co–N(2)–C(6)	106.1(7)	C(2)–N(2)–C(6)	115.3(10)
C(5)–N(2)–C(6)	107.5(9)	N(1)–C(1)–C(2)	104.9(9)
N(2)–C(2)–C(1)	106.1(12)	N(1)–C(3)–C(31)	109.9(9)
N(1)–C(4)–C(41)	105.9(8)	N(2)–C(5)–C(51)	111.2(11)
N(2)–C(6)–C(61)	106.6(10)	Co–N(3)–C(31)	115.6(6)
Co–N(3)–C(35)	126.0(9)	C(31)–N(3)–C(35)	118.3(10)
C(3)–C(31)–N(3)	116.4(10)	C(3)–C(31)–C(32)	119.3(11)
N(3)–C(31)–C(32)	124.1(9)	C(31)–C(32)–C(33)	116.3(13)
C(32)–C(33)–C(34)	121.3(14)	C(33)–C(34)–C(35)	118.9(11)
N(3)–C(35)–C(34)	120.9(12)	Co–N(4)–C(41)	112.8(9)
Co–N(4)–C(45)	126.4(8)	C(41)–N(4)–C(45)	120.7(11)
C(4)–C(41)–N(4)	112.8(11)	C(4)–C(41)–C(42)	126.1(11)
N(4)–C(41)–C(42)	121.1(13)	C(41)–C(42)–C(43)	120.1(13)
C(42)–C(43)–C(44)	117.0(17)	C(43)–C(44)–C(45)	122.7(16)
N(4)–C(45)–C(44)	118.4(10)	Co–N(5)–C(51)	114.8(8)
Co–N(5)–C(55)	127.2(8)	C(51)–N(5)–C(55)	117.9(10)
C(5)–C(51)–N(5)	116.7(10)	C(5)–C(51)–C(52)	121.6(12)
N(5)–C(51)–C(52)	121.6(14)	C(51)–C(52)–C(53)	119.5(14)
C(52)–C(53)–C(54)	119.4(14)	C(53)–C(54)–C(55)	121.1(16)
N(5)–C(55)–C(54)	120.5(13)	Co–N(6)–C(61)	112.6(8)
Co–N(6)–C(65)	129.0(8)	C(61)–N(6)–C(65)	118.4(9)
C(6)–C(61)–N(6)	112.8(9)	C(6)–C(61)–C(62)	127.5(13)
N(6)–C(61)–C(62)	119.6(13)	C(61)–C(62)–C(63)	120.9(15)
C(62)–C(63)–C(64)	119.0(12)	C(63)–C(64)–C(65)	118.8(14)
N(6)–C(65)–C(64)	123.1(12)		

TABLE 8. Atomic Coordinates ($\times 10^4$) for $(-)_{589}$-[Co(tppn)]$(ClO_4)_3$

	x	y	z
Co	8991(1)	5144(1)	4689(1)
N(1)	10368(6)	5591(4)	4079(3)
N(2)	10469(6)	4700(3)	5228(3)
C(1)	11688(7)	5518(4)	4483(5)
C(2)	11733(7)	4768(5)	4748(5)
C(3)	10467(8)	5200(5)	3383(4)
C(4)	9891(9)	6340(4)	3952(4)
C(5)	10682(9)	5060(5)	5926(5)
C(6)	10024(9)	3938(4)	5351(5)
C(7)	13069(12)	4553(8)	5122(9)
N(3)	8875(7)	4401(3)	3944(3)
C(31)	9653(8)	4523(4)	3366(4)
C(32)	9679(10)	4065(6)	2789(5)
C(33)	8830(12)	3459(6)	2789(6)
C(34)	7942(13)	3369(6)	3384(6)
C(35)	8013(9)	3832(4)	3930(5)
N(4)	7791(6)	5703(3)	4083(3)
C(41)	8425(8)	6272(4)	3766(4)
C(42)	7713(12)	6698(5)	3275(5)
C(43)	6396(13)	6532(7)	3092(6)
C(44)	5802(11)	5950(7)	3414(6)
C(45)	6474(8)	5536(5)	3910(4)
N(5)	9019(7)	5898(3)	5422(3)
C(51)	9906(8)	5760(5)	5969(4)
C(52)	10000(11)	6234(6)	6553(5)
C(53)	9187(10)	6823(5)	6579(6)
C(54)	8288(10)	6963(5)	6025(5)
C(55)	8236(8)	6495(4)	5470(5)
N(6)	7892(6)	4576(4)	5346(3)
C(61)	8588(10)	3998(4)	5613(5)
C(62)	8024(13)	3533(6)	6105(5)
C(63)	6642(15)	3649(7)	6301(7)
C(64)	6013(12)	4238(7)	6053(6)
C(65)	6626(8)	4718(5)	5588(4)
Cl(1)	855(3)	3431(1)	726(1)
O(11)	2060(9)	3095(5)	474(5)
O(12)	146(10)	2976(5)	1177(7)
O(13)	1251(16)	4037(5)	1113(6)
O(14)	181(11)	3696(8)	144(6)
Cl(2)	6489(5)	8469(2)	1527(2)
O(21)	7610(12)	8278(4)	1107(5)
O(22)	6643(16)	9163(5)	1758(6)
O(23)	6252(26)	7983(5)	2044(8)
O(24)	5464(17)	8362(11)	1110(13)
Cl(3)	2531(2)	6374(1)	2212(1)
O(31)	3592(10)	6723(5)	1893(7)
O(32)	2649(13)	5637(5)	2197(5)
O(33)	1318(16)	6579(8)	1998(14)
O(34)	2644(10)	6588(7)	2920(6)

TABLE 9. Selected Bond Lengths (A) for $(-)_{589}$-[Co(tppn)]$(ClO_4)_3$

Co–N(1)	1.956(6)	Co–N(2)	1.951(6)
Co–N(3)	1.961(6)	Co–N(4)	1.936(6)
Co–N(5)	1.956(6)	Co–N(6)	1.944(6)
N(1)–C(1)	1.509(10)	N(1)–C(3)	1.494(10)
N(1)–C(4)	1.481(10)	N(2)–C(2)	1.539(10)
N(2)–C(5)	1.481(11)	N(2)–C(6)	1.492(10)
C(1)–C(2)	1.474(12)	C(2)–C(7)	1.542(15)
C(3)–C(31)	1.486(12)	C(4)–C(41)	1.491(12)
C(5)–C(51)	1.504(12)	C(6)–C(61)	1.501(13)
N(3)–C(31)	1.343(10)	N(3)–C(35)	1.352(10)
C(31)–C(32)	1.373(13)	C(32)–C(33)	1.398(16)
C(33)–C(34)	1.425(16)	C(34)–C(35)	1.334(14)
N(4)–C(41)	1.360(10)	N(4)–C(45)	1.372(10)
C(41)–C(42)	1.397(13)	C(42)–C(43)	1.376(17)
C(43)–C(44)	1.364(17)	C(44)–C(45)	1.374(14)
N(5)–C(51)	1.371(10)	N(5)–C(55)	1.348(10)
C(51)–C(52)	1.403(14)	C(52)–C(53)	1.352(15)
C(53)–C(54)	1.387(14)	C(54)–C(55)	1.353(13)
N(6)–C(61)	1.364(11)	N(6)–C(65)	1.353(10)
C(61)–C(62)	1.376(14)	C(62)–C(63)	1.425(19)
C(63)–C(64)	1.336(19)	C(64)–C(65)	1.382(15)

in the plane of, and opposite to, the ethylenediamine ring and is the most strained angle in the octahedron. The L_G–Co–L_G angles of $[Co(tppn)]^{3+}$, $[Co(tpen)]^{3+}$, $[Co(edampda)]^{+}$, $[Co(edta)]^{-}$, $[Co(penten)]^{3+}$ and $[Co(\ell\text{-mepenten})]^{3+}$ are 108.5(3)°, 108.2(4)°, 107.0(1)°, 104.1(7)°, 102.2(6)° and 103(1)°, respectively. As expected, the tppn and tpen complexes have the largest angles; $[Co(edampda)]^{+}$ is intermediate between $[Co(edta)]^{-}$ and $[Co(tpen)]^{3+}$; and the penten and ℓ-mepenten complexes have the smallest angles.

The strain in both $[Co(tpen)]^{3+}$ and $[Co(tppn)]^{3+}$ is large enough to distort their octahedra in two opposite directions. For $[Co(tpen)]^{3+}$, the ligand–cobalt–ligand (L–Co–L) angles in the face N1–N3–N4 are all acute, and the L–Co–L angles in the opposite face, N2–N5–N6, are also all acute. As expected, the L–Co–L angles outside of these faces (N1–Co–N5, N4–Co–N5, and N2–Co–N3, N3–Co–N6) are all obtuse. This high degree of octahedral strain is not observed in the edampda, edta, penten or ℓ-mepenten cobalt complexes.

An indication of the induced planarity in the G pyridyl arms of $[Co(edampda)]^{+}$, $[Co(tpen)]^{3+}$ and $[Co(tppn)]^{3+}$ is obtained from an analysis of torsion angles within the G arms of the complexes included in this study. For example, in arm G_1 of the edampda complex, the torsion angle N4–Co–N2–C7, that measures the extent of puckering in the inner region of the G chelate ring, is 36.9(1)°. Torsion angle Co–N4–C41–C7, that measures the extent of puckering in the outer region of the same G chelate ring, is 2.2(2)°. Comparison of these torsion angles of the edampda complex to the analogous torsion angles of the G rings of the other complexes in this study shows that the magnitude of the torsion angle that measures puckering in the inner chelate ring is greater than 33° for all six complexes (e.g. O7–Co–N2–C7 is −37.4° for

TABLE 10. Selected Bond Angles (°) for $(-)_{589}$-[Co(tppn)]$(ClO_4)_3$

N(1)–Co–N(2)	87.8(3)	N(1)–Co–N(3)	85.5(3)
N(2)–Co–N(3)	96.7(3)	N(1)–Co–N(4)	81.7(3)
N(2)–Co–N(4)	169.1(3)	N(3)–Co–N(4)	85.5(3)
N(1)–Co–N(5)	95.6(3)	N(2)–Co–N(5)	85.8(3)
N(3)–Co–N(5)	177.3(3)	N(4)–Co–N(5)	92.2(3)
N(1)–Co–N(6)	169.3(3)	N(2)–Co–N(6)	82.1(3)
N(3)–Co–N(6)	92.2(3)	N(4)–Co–N(6)	108.6(3)
N(5)–Co–N(6)	87.1(3)	Co–N(1)–C(1)	105.5(5)
Co–N(1)–C(3)	110.4(5)	C(1)–N(1)–C(3)	109.7(6)
Co–N(1)–C(4)	105.6(5)	C(1)–N(1)–C(4)	116.0(6)
C(3)–N(1)–C(4)	109.5(6)	Co–N(2)–C(2)	105.6(5)
Co–N(2)–C(5)	111.9(5)	C(2)–N(2)–C(5)	111.2(6)
Co–N(2)–C(6)	104.9(5)	C(2)–N(2)–C(6)	113.8(6)
C(5)–N(2)–C(6)	109.2(6)	N(1)–C(1)–C(2)	106.2(6)
N(2)–C(2)–C(1)	104.4(6)	N(2)–C(2)–C(7)	113.9(8)
C(1)–C(2)–C(7)	114.8(8)	N(1)–C(3)–C(31)	113.0(7)
N(1)–C(4)–C(41)	105.4(6)	N(2)–C(5)–C(51)	111.2(7)
N(2)–C(6)–C(61)	104.9(6)	Co–N(3)–C(31)	114.9(5)
Co–N(3)–C(35)	126.5(6)	C(31)–N(3)–C(35)	118.3(7)
C(3)–C(31)–N(3)	115.6(7)	C(3)–C(31)–C(32)	121.7(8)
N(3)–C(31)–C(32)	122.7(8)	C(31)–C(32)–C(33)	118.8(9)
C(32)–C(33)–C(34)	117.5(10)	C(33)–C(34)–C(35)	119.4(10)
N(3)–C(35)–C(34)	123.1(9)	Co–N(4)–C(41)	112.9(5)
Co–N(4)–C(45)	126.5(6)	C(41)–N(4)–C(45)	120.4(7)
C(4)–C(41)–N(4)	114.1(7)	C(4)–C(41)–C(42)	126.3(8)
N(4)–C(41)–C(42)	119.5(8)	C(41)–C(42)–C(43)	120.7(9)
C(42)–C(43)–C(44)	118.0(10)	C(43)–C(44)–C(45)	122.1(10)
N(4)–C(45)–C(44)	119.3(9)	Co–N(5)–C(51)	113.5(5)
Co–N(5)–C(55)	128.5(5)	C(51)–N(5)–C(55)	117.9(7)
C(5)–C(51)–N(5)	116.4(7)	C(5)–C(51)–C(52)	123.1(8)
N(5)–C(51)–C(52)	120.4(8)	C(51)–C(52)–C(53)	119.5(9)
C(52)–C(53)–C(54)	120.1(9)	C(53)–C(54)–C(55)	118.5(9)
N(5)–C(55)–C(54)	123.6(8)	Co–N(6)–C(61)	112.0(5)
Co–N(6)–C(65)	128.3(6)	C(61)–N(6)–C(65)	119.5(7)
C(6)–C(61)–N(6)	114.3(7)	C(6)–C(61)–C(62)	123.5(9)
N(6)–C(61)–C(62)	122.1(9)	C(61)–C(62)–C(63)	117.7(10)
C(62)–C(63)–C(64)	118.4(12)	C(63)–C(64)–C(65)	122.6(11)
N(6)–C(65)–C(64)	119.3(9)		

TABLE 11. Atomic Coordinates ($\times 10^4$) for [Cu(*uns*-Hpenp)-Cl_2]ClO_4

	x	*y*	*z*
Cu	297(1)	2401(1)	2500
Cl(1)	−1135(1)	1230(2)	2500
Cl(2)	24(1)	5419(2)	2500
N(2)	1541(3)	1275(6)	2500
N(1)	2963(5)	5208(8)	2396
C(1)	2302(6)	3890(11)	2054(6)
C(2)	2273(5)	2509(10)	2700
C(3)	1572(4)	210(6)	1680(3)
N(3)	452(2)	2148(4)	1200(3)
C(31)	1078(3)	1110(5)	937(3)
C(32)	1226(3)	753(6)	39(4)
C(33)	706(3)	1544(6)	−595(3)
C(34)	60(4)	2661(6)	−317(3)
C(35)	−51(3)	2938(6)	585(3)
Cl(3)	2500	5888(2)	5000
O(1)	2657(6)	6964(8)	5724(4)
O(2)	1788(4)	4877(6)	5193(5)

TABLE 12. Selected Bond Lengths (Å) for [Cu(*uns*-Hpenp)-Cl_2]ClO_4

Cu–Cl(1)	2.370(2)	Cu–Cl(2)	2.434(2)
Cu–N(2)	2.094(5)	Cu–N(3)	1.968(4)
Cu–N(3a)	1.968(4)	N(2)–C(2)	1.515(9)
N(2)–C(3)	1.490(6)	N(2)–C(2a)	1.514(9)
N(2)–C(3a)	1.490(6)	N(1)–C(1)	1.539(11)
C(1)–C(2)	1.462(11)	N(3)–C(31)	1.320(6)
C(3)–C(31)	1.521(7)	C(31)–C(32)	1.391(7)
N(3)–C(35)	1.351(6)	C(33)–C(34)	1.388(7)
C(32)–C(33)	1.385(7)		
C(34)–C(35)	1.377(7)		

TABLE 13. Selected Bond Angles (°) for [Cu(*uns*-Hpenp)Cl_2]ClO_4

Cl(1)–Cu–Cl(2)	103.3(1)	Cl(1)–Cu–N(2)	131.6(1)
Cl(2)–Cu–N(2)	125.1(1)	Cl(1)–Cu–N(3)	94.0(1)
Cl(2)–Cu–N(3)	96.9(1)	N(2)–Cu–N(3)	81.3(1)
Cl(1)–Cu–N(3a)	94.0(1)	Cl(2)–Cu–N(3a)	96.9(1)
N(2)–Cu–N(3a)	81.3(1)	N(3)–Cu–N(3a)	161.9(2)
Cu–N(2)–C(2)	112.9(4)	Cu–N(2)–C(3)	105.7(3)
C(2)–N(2)–C(3)	120.5(4)	Cu–N(2)–C(2a)	112.9(4)
C(2)–N(2)–C(2a)	22.8(1)	C(3)–N(2)–C(2a)	100.5(3)
Cu–N(2)–C(3a)	105.7(3)	C(2)–N(2)–C(3a)	100.5(3)
C(3)–N(2)–C(3a)	110.7(5)	N(1)–C(1)–C(2)	108.1(6)
N(2)–C(2)–C(1)	112.2(5)	N(2)–C(3–C(31)	108.6(4)
Cu–N(3)–C(31)	116.4(3)	Cu–N(3)–C(35)	123.9(3)
C(31)–N(3)–C(35)	119.8(4)	C(3)–C(31)–N(3)	115.7(4)
C(3)–C(31)–C(32)	122.0(4)	N(3)–C(31)–C(32)	122.1(4)
C(31)–C(32)–C(33)	118.4(5)	C(32)–C(33)–C(34)	119.3(5)
C(33)–C(34)–C(35)	118.8(5)	N(3)–C(35)–C(34)	121.6(5)

TABLE 14. Atomic Coordinates ($\times 10^4$) for tppn

	x	*y*	*z*
N(2)	−939(5)	7610(3)	4411(3)
N(1)	−304(6)	5561(4)	1697(3)
C(2)	210(7)	6496(4)	3680(4)
C(1)	−1241(7)	6637(4)	2501(4)
C(5)	−137(7)	7179(4)	5760(3)
C(6)	−862(7)	9139(3)	3857(4)
C(3)	−477(7)	4080(4)	2309(4)
C(4)	−1364(7)	6028(4)	403(4)
C(7)	2551(7)	6532(5)	3315(4)
N(5)	649(6)	4754(3)	7142(3)
C(51)	−912(7)	5941(4)	6556(4)
C(52)	−3156(7)	6027(4)	6682(4)
C(53)	−3772(8)	4898(5)	7462(4)
C(54)	−2181(8)	3664(5)	8109(4)
C(55)	−2(9)	3649(5)	7894(4)
N(6)	−1867(6)	11367(3)	4694(3)
C(61)	−2582(6)	10261(4)	4390(3)
C(62)	−4761(7)	10204(5)	4518(4)
C(63)	−6283(8)	11296(4)	4982(4)
C(64)	−5578(9)	12404(5)	5314(4)
C(65)	−3372(8)	12440(4)	5147(4)
N(3)	3254(7)	2831(4)	1555(4)
C(31)	1025(6)	2868(4)	1702(3)
C(32)	159(6)	1882(3)	1394(3)
C(33)	1504(9)	811(5)	943(4)
C(34)	3739(8)	632(4)	766(4)
C(35)	4607(7)	1684(4)	1049(4)
N(4)	−2232(6)	8475(3)	−1028(3)
C(41)	−647(7)	7298(5)	−421(4)
C(42)	1586(7)	7197(5)	−598(4)
C(43)	2221(8)	8342(5)	−1399(4)
C(44)	542(9)	9530(5)	−2016(4)
C(45)	−1589(8)	9561(4)	−1797(4)

TABLE 15. Selected Bond Lengths (Å) for tppn

N(2)–C(2)	1.471(5)	N(2)–C(5)	1.465(5)
N(2)–C(6)	1.471(5)	N(1)–C(1)	1.468(6)
N(1)–C(3)	1.461(5)	N(1)–C(4)	1.465(5)
C(2)–C(1)	1.524(6)	C(2)–C(7)	1.515(6)
C(5)–C(51)	1.493(6)	C(6)–C(61)	1.495(5)
C(3)–C(31)	1.530(5)	C(4)–C(41)	1.509(6)
N(5)–C(51)	1.325(4)	N(5) C(55)	1.338(6)
C(51)–C(52)	1.389(6)	C(52)–C(53)	1.357(6)
C(53)–C(54)	1.380(6)	C(54)–C(55)	1.374(8)
N(6)–C(61)	1.353(6)	N(6)–C(65)	1.356(5)
C(61)–C(62)	1.382(6)	C(62)–C(63)	1.378(6)
C(63)–C(64)	1.364(7)	C(64)–C(65)	1.397(7)
N(3)–C(31)	1.392(6)	N(3)–C(35)	1.391(6)
C(31)–C(32)	1.307(6)	C(32)–C(33)	1.307(5)
C(33)–C(34)	1.375(7)	C(34)–C(35)	1.354(7)
N(4)–C(41)	1.335(5)	N(4)–C(45)	1.329(5)
C(41)–C(42)	1.386(6)	C(42)–C(43)	1.383(6)
C(43)–C(44)	1.375(6)	C(44)–C(45)	1.342(8)

arm G_2 of the edta complex) but that the magnitude of the torsion angle which measures puckering in the outer chelate ring is at least nine degrees for non-pyridyl G rings and less than five degrees for pyridyl G rings (e.g. C7–C8–O7–Co is −16.5° for arm G_2 of the edta complex). The related torsion angles are listed in Table 19.

The bond lengths of the edampda, tpen and tppn cobalt complexes are all similar to those reported for other amine cobalt complexes. The bond lengths and bond angles in the organic tppn structure are all similar to those reported for other organic structures.

The absolute configuration of the $[Co(tppn)]^{3+}$ complex was determined via collection of the Friedel pairs listed in Table 20. The differences in intensity between the reflections and the counter-reflections is clearly observable. Comparison of the observed and calculated differences shows that $(-)_{589}$-$[Co(tppn)]^{3+}$ has the absolute configuration designated as skew chelate pairs ΔΛΔ [13].

TABLE 16. Selected Bond Angles (°) for tppn

C(2)–N(2)–C(5)	111.2(3)	C(2)–N(2)–C(6)	114.9(3)
C(5)–N(2)–C(6)	110.1(3)	C(1)–N(1)–C(3)	111.0(3)
C(1)–N(1)–C(4)	111.7(3)	C(3)–N(1)–C(4)	110.4(4)
N(2)–C(2)–C(1)	108.8(3)	N(2)–C(2)–C(7)	115.3(4)
C(1)–C(2)–C(7)	111.5(3)	N(1)–C(1)–C(2)	114.4(3)
N(2)–C(5)–C(51)	114.7(4)	N(2)–C(6)–C(61)	112.1(3)
N(1)–C(3)–C(31)	112.1(3)	N(1)–C(4)–C(41)	112.6(4)
C(51)–N(5)–C(55)	117.8(4)	C(5)–C(51)–N(5)	116.6(4)
C(5)–C(51)–C(52)	121.8(3)	N(5)–C(51)–C(52)	121.5(4)
C(51)–C(52)–C(53)	119.4(4)	C(52)–C(53)–C(54)	120.2(5)
C(53)–C(54)–C(55)	116.5(4)	N(5)–C(55)–C(54)	124.4(4)
C(61)–N(6)–C(65)	117.6(4)	C(6)–C(61)–N(6)	115.0(3)
C(6)–C(61)–C(62)	122.5(4)	N(6)–C(61)–C(62)	122.5(3)
C(61)–C(62)–C(63)	119.7(4)	C(62)–C(63)–C(64)	118.5(5)
C(63)–C(64)–C(65)	120.2(4)	N(6)–C(65)–C(64)	121.6(4)
C(31)–N(3)–C(35)	117.7(4)	C(3)–C(31)–N(3)	118.8(4)
C(3)–C(31)–C(32)	117.9(4)	N(3)–C(31)–C(32)	123.3(4)
C(31)–C(32)–C(33)	116.7(4)	C(32)–C(33)–C(34)	126.0(5)
C(33)–C(34)–C(35)	116.9(4)	N(3)–C(35)–C(34)	119.3(4)
C(41)–N(4)–C(45)	117.4(4)	C(4)–C(41)–N(4)	117.7(4)
C(4)–C(41)–C(42)	120.7(3)	N(4)–C(41)–C(42)	121.5(4)
C(41)–C(42)–C(43)	120.2(4)	C(42)–C(43)–C(44)	116.7(5)
C(43)–C(44)–C(45)	120.1(4)	N(4)–C(45)–C(44)	124.1(4)

The circular dichroism (CD) spectrum of $(-)_{589}$-$[Co(tppn)]^{3+}$ clearly shows three transitions at 381, 450 and 500 nm [6]. All three transitions have negative Cotton effects. It is now possible to draw an unequivocal correlation between the negative signs of the CD transitions in hexadentate polypyridyl cobalt complexes and the absolute configuration ΔΛΔ.

In addition, it is now possible to identify the optical isomer of $[Co(tpen)]^{3+}$ that was reported in our previous work [6]. The CD spectrum of this optical isomer clearly showed three transitions at 381, 450 and 500 nm. In this case, all three transitions had positive Cotton effects. By analogy, this optical isomer of $[Co(tpen)]^{3+}$ has the absolute configuration designated as skew chelate pairs ΛΔΛ.

The determination of the [Cu(*uns*-Hpenp)Cl_2]-ClO_4 structure unambiguously assigns the penp ligand as the novel unsymmetrical geometrical isomer, *uns*-penp (*uns*-penp is *N,N*-bis(2-pyridylmethyl)ethylenediamine). This assignment agrees with the previously documented synthetic route and the coupling constant of 16 Hz reported for the R pyridyl arms in [Co(*uns*-penp)(H_2O)Cl]-$(ClO_4)_2$ [6]. (If the cobalt complex had contained the symmetrical penp isomer, the coupling constant of the *trans* R pyridyl arms would have been 18–19 Hz.)

The N3(py)–Cu and N2–Cu bond lengths of the Cu *uns*-penp complex are very close to the previously reported [14], analogous bond lengths of $[Cu(N_3S)Br]ClO_4$ (N_3S is *N,N*-bis(2-pyridylmethyl)-*N*-(2-methylthioethyl)amine). In addition, the Cu–halogen bond lengths in these two complexes are similar. The two structures are similar even though $[Cu(uns\text{-}Hpenp)Cl_2]^+$ has distorted trigonal bipyramidal geometry and $[Cu(N_3S)Br]^+$ has distorted square pyramidal geometry. The common structural features that influence the bond lengths of these two complexes are two pyridyl arms bonded *trans* to each other, an aliphatic nitrogen in the same plane that contains both pyridine rings, and a pendant ligand arm. All other bond lengths and angles of $[Cu(uns\text{-}Hpenp)Cl_2]^+$ agree with the data of the other complexes reported in this work.

The ring angle sums of the two crystallographically-equivalent pyridyl arms in the Cu *uns*-Hpenp complex produce a Δ value of 21.3(0.7)°. This shows the expected level of strain which is intermediate between the strain of R and G rings of hexadentate polypyridyl ligands that are bonded to metal centers.

Supplementary Material

Tables of all atomic coordinates, all bond lengths, all bond angles, anisotropic temperature factors, H atom coordinates with isotropic temperature factors, torsion angles, least-squares planes, structure factors, structure factors of the Friedel pairs, and rigid-body thermal vibration data are available from the author upon request.

TABLE 17. Ring Angle Sum Deviations from Ideal Ring Angle Sums in Cobalt Complexes of Hexadentate Ligands[a]

Ring	[Co(penten)]$^{3+}$	[Co(ℓ-mepenten)]$^{3+}$	[Co(edta)]$^{-}$	[Co(edampda)]$^{+}$	[Co(tpen)]$^{3+}$	[Co(tppn)]$^{3+}$
R_1	7.0(2.8)(N9–N11)	4.0(4.9)(N9–N11)	0.7(2.0)(N1–O8)	0.7(0.3)(N1–O1)	10.0(2.0)(N2–N5)	10.2(1.2)(N2–N5)
R_2	1.4(2.6)(N8–N12)	18.0(5.2)(N8–N12)	0.7(2.0)(N2–O6)	−0.2(0.3)(N2–O3)	9.9(1.6)(N1–N3)	9.6(1.3)(N1–N3)
E	8.2(2.9)(N8–N9)	11.0(4.7)(N8–N9)	7.0(2.0)(N1–N2)	12.0(0.3)(N1–N2)	16.4(1.8)(N1–N2)	18.5(1.1)(N1–N2)
G_1	6.7(2.9)(N9–N10)	13.0(4.9)(N7–N8)	14.4(2.0)(N1–O5)	27.3(0.3)(N2–N4)	29.8(1.8)(N1–N4)	29.0(1.2)(N1–N4)
G_2	10.9(2.9)(N7–N8)	13.0(5.4)(N9–N10)	15.3(2.0)(N2–O7)	27.4(0.4)(N1–N3)	28.8(1.8)(N2–N6)	30.8(1.2)(N2–N6)

[a]Ligating atoms of each ring are identified. Angles are in degrees.

TABLE 18. Root-mean-square Deviations of Atoms from Least-squares Planes in Cobalt Complexes of Hexadentate Ligands[a]

Ring	[Co(penten)]$^{3+}$	[Co(ℓ-mepenten)]$^{3+}$	[Co(edta)]$^{-}$	[Co(edampda)]$^{+}$	[Co(tpen)]$^{3+}$	[Co(tppn)]$^{3+}$
R_1	0.1938	0.1719	0.0676	0.0711	0.0516	0.0512
R_2	0.1535	0.2375	0.0718	0.0563	0.0404	0.0351
E	0.1937	0.2043	0.1826	0.2031	0.2195	0.2279
G_1	0.2009	0.2224	0.1988	0.2067	0.2169	0.2167
G_2	0.2395	0.2251	0.2073	0.2104	0.2124	0.2257

[a]Ligating atoms are identified in Table 17.

TABLE 19. Torsion Angles in G Rings of Cobalt Complexes of Hexadentate Ligands

Complex	Ring	Torsion angle	(°)
$[Co(edampda)]^+$	G_1	N4–Co–N2–C7	36.9
	G_1	Co–N4–C41–C7	2.2
	G_2	N3–Co–N1–C8	37.7
	G_2	Co–N3–C31–C8	4.5
$[Co(tpen)]^{3+}$	G_1	N4–Co–N1–C4	38.2
	G_1	Co–N4–C41–C4	−1.4
	G_2	N6–Co–N2–C6	38.1
	G_2	Co–N6–C61–C6	1.0
$[Co(tppn)]^{3+}$	G_1	N4–Co–N1–C4	38.4
	G_1	Co–N4–C41–C4	0.1
	G_2	N6–Co–N2–C6	39.9
	G_2	Co–N6–C61–C6	0.8
$[Co(edta)]^-$	G_1	O7–Co–N2–C7	−37.4
	G_1	C7–C8–O7–Co	−16.5
	G_2	O5–Co–N1–C3	−35.1
	G_2	C3–C4–O5–Co	−9.2
$[Co(penten)]^{3+}$	G_1	N10–Co–N9–C11	−33.6
	G_1	Co–N10–C12–C11	9.4
	G_2	N7–Co–N8–N9	−44.1
	G_2	Co–N7–C10–C9	−9.2
$[Co(\ell\text{-mepenten})]^{3+}$	G_1	N7–Co–N8–C9	36.8
	G_1	Co–N7–C10–C9	−19.0
	G_2	N10–Co–N9–C11	35.7
	G_2	Co–N10–C12–C11	−19.6

TABLE 20. Determination of the Absolute Configuration of $[Co(tppn)]^{3+}$

Indices	$F_c^2(hkl)$ $\times 10^{-2}$	Observed relations	$F_c^2(\bar{h}\bar{k}\bar{l})$ $\times 10^{-2}$
2 2 1	150.3	<	213.7
1 2 5	168.7	>	130.4
8 1 7	6.97	>	1.14
1 1 3	257.9	<	309.4
1 5 3	64.1	>	42.3
5 5 3	14.3	<	27.7
2 1 3	69.4	>	49.8
3 2 4	42.6	>	27.6
5 3 1	77.1	<	102.0
1 2 8	10.2	<	17.5
3 2 6	84.0	>	59.0
9 2 7	1.17	<	5.20
6 5 8	0.14	<	2.7
1 7 3	25.8	<	42.0
1 3 3	112.1	<	142.8
5 1 15	5.86	>	1.10
2 6 3	12.7	<	24.2
1 4 5	6.42	>	1.90
4 4 2	13.2	<	22.3
2 11 2	25.0	>	15.0
5 11 8	3.96	>	1.56
3 4 6	48.0	>	32.5
1 2 6	35.5	<	50.3
2 5 9	15.7	>	9.99
3 3 12	2.62	<	6.92
3 4 8	28.9	<	41.6
3 11 7	1.59	<	6.00

Acknowledgements

The authors thank Professor Bryan M. Craven of the University of Pittsburgh, Department of Crystallography, for his assistance and advice. The X-ray structure analysis was carried out in the Department of Chemistry X-ray Laboratory directed by J. E. Abola under support of Public Health Service Grant 1-S10-RR02381-01. Structure 1 was refined by Dr Abola.

References

1 P. Arslan, F. DiVirgilio, M. Beltrame, R. Y. Tsien and T. Pozzan, *J. Biol. Chem., 260* (1985) 2719.
2 J. H. Doroshow, *Biochem. Biophys. Res. Commun., 135* (1986) 330.
3 R. R. Gagne, R. P. Kreh, J. A. Dodge, R. E. Marsh and M. McCool, *Inorg. Chem., 21* (1982) 254.
4 B. F. Hoskins and F. D. Whillans, *J. Chem. Soc., Dalton Trans.*, (1975) 657.
5 K. D. Karlin, J. C. Hayes, S. Juen, J. P. Hutchinson and J. Zubieta, *Inorg. Chem., 21* (1982) 4106.
6 J. B. Mandel, C. Maricondi and B. E. Douglas, *Inorg. Chem., 27* (1988) 2990.
7 *International Tables of X-Ray Crystallography*, Vol. IV, Kynoch, Birmingham, U.K., 1974.
8 V. Schomaker and K. N. Trueblood, *Acta Crystallogr., Sect. B, 24* (1968) 63.
9 B. M. Craven, *Program 'FLAP'*, Department of Crystallography, University of Pittsburgh, PA, 1982.
10 H. A. Weakliem and J. L. Hoard, *J. Am. Chem. Soc., 81* (1959) 549.
11 A. Muto, M. Fumiyuki and Y. Saito, *Acta Crystallogr., Sect. B, 26* (1970) 226.
12 A. Kobayashi, F. Marumo and Y. Saito, *Acta Crystallogr., Sect. B, 30* (1974) 1495.
13 The IUPAC rules, *Inorg. Chem., 9* (1970) 1.
14 Y. Nishida and K. Takahashi, *Inorg. Chem., 27* (1988) 1406.